Development and calibration of a model for the potential establishment and impact of *Aedes albopictus* in Europe

S. Pasquali[1], L. Mariani[2,3], M. Calvitti[4], R. Moretti[4], L. Ponti[4,5], M. Chiari[6], G. Sperandio[7,8], G. Gilioli[7]

[1] CNR-IMATI "Enrico Magenes", Via A. Corti 12, 20133 Milano, Italy

[2] Lombard Museum of Agricultural History, Via Celoria, 2, 20133 Milano, Italy

[3] DiSAA, Università degli Studi di Milano, Via Celoria 2, 20133 Milano, Italy

[4] Biotechnology and Agroindustry Division, ENEA (Italian National Agency for New Technologies, Energy and Sustainable Economic Development), Casaccia Research Center, via Anguillarese 301, 00123 Rome, Italy

[5] Center for the Analysis of Sustainable Agricultural Systems (www.casasglobal.org), Kensington CA 94707, USA

[6] UO Veterinaria, DG Welfare, Regione Lombardia, P.zza Città di Lombardia 1, 20124 Milano, Italy

[7] DMMT, University of Brescia, Viale Europa 11, 25123 Brescia, Italy

[8] Department of Life Sciences, University of Modena and Reggio Emilia, Via G. Amendola 2, 42122 Reggio Emilia, Italy

Abstract

The Asian tiger mosquito (*Aedes albopictus*) is one of the most invasive disease vectors worldwide. The species is a competent vector of dengue, chikungunya, Zika viruses and other severe parasites and pathogens threatening human health. The capacity of this mosquito to colonize and establish in new areas (including temperate regions) is enhanced by its ability of producing diapausing eggs that survive relatively cold winters. The main drivers of population dynamics for this mosquito are water and air temperature and

photoperiod. In this paper, we present a mechanistic model that predicts the potential distribution, abundance and activity of Asian tiger mosquito in Europe. The model includes a comprehensive description of: i) the individual life-history strategies, including diapause, ii) the influence of weather-driven individual physiological responses on population dynamics and iii) the density-dependent regulation of larval mortality rate. The model is calibrated using field data from several locations along an altitudinal gradient in the Italian Alps, which enabled accurate prediction of cold temperature effects on population abundance, including identification of conditions that prevent overwintering of the species. Model predictions are consistent with the most updated information on species' presence and absence. Predicted population abundance shows a clear south-north decreasing gradient. A similar yet less evident pattern in the activity of the species is also predicted. The model represents a valuable tool for the development of strategies aimed at the management of *Ae. albopictus* and for the implementation of effective control measures against vector-borne diseases in Europe.

Keywords: population dynamics, *Ae. albopictus*, stage-structured population, demographic model

1. Introduction

The Asian tiger mosquito, *Aedes albopictus* (Skuse, 1894) (Diptera: Culicidae), is one of the most invasive disease vectors worldwide (Benedict et al., 2007; Medlock et al., 2012; Paupy et al., 2009). In less than 40 years, this species has spread from its native distribution area (southeast Asia) to all inhabited continents (Knudsen, 1995; Kraemer et al., 2015; Moore and Mitchell, 1997). Since the first finding of *Ae. albopictus* in Europe, recorded in Albania in 1979 (Adhami, 1998), the mosquito rapidly established in southern and central Europe in the following decades (Medlock et al., 2012) reaching Germany (Kulisch et al al., 2018) and Czech Republic (Rudolf et al., 2018). The dispersal of this species across continents is due to passive transportation of eggs via the global trade of used tires or other materials in which eggs can be laid and survive (Reiter and Sprenger, 1987). Once established, the dispersal of adult individuals is facilitated by passive ground transportation (Medlock et al., 2012; Rudolf et al., 2018). The success of *Ae. albopictus* in

establishing in temperate latitudes is due to the capacity of producing diapausing eggs able to survive relatively cold winters (Benedict et al., 2007; Kuhlisch et al., 2018; Reiter, 1998). The Asian tiger mosquito has been recognized as competent vector for a range of severe human pathogens and parasites among which dengue, chikungunya, Zika and occasionally west Nile viruses (Couto-Lima et al., 2017; Gratz, 2004; Guo et al., 2013; Leta et al., 2018; Paupy et al., 2009; Shragai et al., 2017; Stanaway et al., 2016) becoming responsible of a growing public health concern. The recent autochthonous outbreaks of chikungunya and dengue in the European Mediterranean area (Angelini et al., 2007; Gjenero-Margan et al., 2011; La Ruche et al., 2010; Manica et al., 2017) underlined the urgent need of developing new strategies for evaluating the risks of transmission of emerging pathogens in not autochthonous epidemiological niches. These strategies include rigorous monitoring systems and tools describing the phenology and the population dynamics of the mosquito in the current and in the potential area of distribution (Fischer et al., 2014).

Several studies have tried to define the area of potential distribution, abundance or habitat suitability of *Ae. albopictus* throughout the development of models coupled with Geographic Information Systems (GIS) considering the influence of environmental and climatic variables (for a review, see Fischer et al. (2014)). Among others, temperature, photoperiod and precipitation patterns have been identified as the most influencing drivers in determining the mosquito habitat suitability (Brady et al., 2013; Campbell et al., 2015; Sallam et al., 2017; Tran et al., 2013).

The modelling approaches used for predicting the potential distribution of *Ae. albopictus* mainly refer to correlative (statistical) and mechanistic approaches. Correlative models are based on investigating the correlation existing between one or more variables and the current occurrence of the species. The main outputs of these models refers to species habitat suitability or potential spatial distribution (Benedict et al., 2007; Ding et al., 2018; Kraemer et al., 2019; Proestos et al., 2015; Santos and Mesenes, 2017; Sanz-Aguilar et al., 2018; Trájer et al., 2014). Despite their wide use, correlative approaches might have some limitations in predicting the potential distribution of the investigated species. The lack of exhaustive presence-absence datasets and difficulties in interpreting the real area of distribution (e.g. misidentification of the species, presence of transient populations, ongoing spread in new areas etc.) might lead to wrong interpretation of

the habitat suitability of the species (Kobayashi et al., 2002; Soberón and Peterson, 2011). Furthermore, these modelling approaches do not provide information on species potential abundance and impacts in the assessed area. The interpretation of habitat suitability indexes in the context of risk assessment is problematic, since the meaning of these indexes cannot be interpreted in terms of population abundance neither in any other variable directly related to the impact of a vector. On the other hand, mechanistic models do not require full datasets of presence-absence records, since they are able to predict the population dynamics based on individual traits and physiological responses to environmental driving variables. Furthermore, these types of models allow predicting the potential species population abundance, thus providing a direct link to the impacts of that species in the assessed area (Erguler et al., 2016; Gilioli et al., 2014; Gutierrez, 1996; Gutierrez and Ponti, 2013). Projections of vector population abundance can also account for individual variability and non-linearity in the responses to environmental drivers (Soberón and Nakamura, 2009). A complete overview on the main differences between mechanistic and statistical modelling approaches applied to *Ae. albopictus* is presented in Brady et al. (2014) and Fischer et al. (2014). The first mechanistic models were based on the selection of relevant variables (mean temperature in January, annual rainfall, photoperiod etc.) used for setting up climatic constraints for predicting the areas of potential establishment and mosquito seasonal activity (ECDC, 2009; Kobayashi et al., 2002; Medlock et al., 2006). These models were used for simulating *Ae. albopictus* climate suitability and seasonal activity locally (Petrić et al., 2017) and at European level (Caminade et al., 2012).

The first stage-structured model simulating *Ae. albopictus* local population dynamics was developed by Erickson et al. (2010). Subsequent developments referred to the implementation of mechanistic models of vector dynamics coupled with a model for the disease dynamics for the assessment of vector-borne disease epidemics (Erguler et al., 2017; Erickson et al., 2012; Guzzetta et al., 2016a,b; Mordecai et al., 2017; Poletti et al., 2011). Other mechanistic models included the influence of diapause on inter-annual mosquito population dynamics (Erguler et al., 2016, 2017; Jia et al., 2016; Tran et al., 2013; Zheng et al., 2018). Some models included also the potential role of climate change on mosquito population dynamics (Gilioli et al., 2015; Jia et al., 2017) and on habitat suitability (Metelmann et al., 2019).

99 In this paper, we present a weather-driven, spatially-explicit, mechanistic model based on a system of partial
100 differential equations. The model gives a comprehensive description of the individual life-history strategies,
101 including diapause, taking into account the role of biotic interaction on mosquito population dynamics
102 throughout the application of density-dependent mortality of larvae.
103 The estimation of parameters referring to larval density-dependent mortality is performed using average
104 egg counts obtained by ovitrap captures in seven locations of the Bolzano Province (Italy) following an
105 altitudinal gradient. Other parameters linked to development, mortality and fecundity of *Ae. albopictus* are
106 estimated separately by fitting functions to experimental data collected from literature.

107 The aim of our work is to predict: i) the area of potential establishment, ii) the potential population
108 abundance iii) the seasonal population activity (expressed as the number of weeks between the spring egg
109 hatching and the beginning of autumn egg diapause) of *Ae. albopictus* females in Europe. Predicted
110 population abundance and seasonal population activity can be regarded as proxies of the species habitat
111 suitability or alternatively, they can be used to infer the potential impact of *Ae. albopictus* in the assessed
112 area.

113 The paper is organized as follows: in Section 2 we describe the demographic model for *Ae. albopictus*; in
114 Section 3 we present the methodology followed to generate weather data, and data on eggs abundance used
115 for model calibration; in Section 4 we present the results of the calibration procedure and the maps
116 representing the area of potential distribution, abundance and activity of *Ae. albopictus* in Europe; in
117 Section 5 we discuss the main results and provide concluding remarks.

118 **2. The mathematical model**

119

120 The population dynamics of *Ae. albopicuts* is represented by a system of Fokker-Planck partial differential
121 equations, already presented in Buffoni and Pasquali (2007). It is a stage-structured demographic model

that has been applied to other species in Gilioli et al. (2014, 2016, 2017a,b,c), and Lanzarone et al. (2017), and also in Pasquali et al. (2019) in its simplified form of phenological model.

Assume the population composed by s stages. Denote by $\phi^i(t,x)$ $(i = 1,2,3,4)$ the abundance of individuals in stage i $(i = 1,2,\dots,s)$ at time *t,* with physiological age *x*, that is the percentage of development of an individual in a stage. Let $v^i(t)$ and $m^i(t)$ be the stage-specific development and mortality rates, respectively. The population dynamics is described by the system:

$$\frac{\partial \phi^i}{\partial t} + \frac{\partial}{\partial x}\left[v^i(t)\phi^i - \sigma^i \frac{\partial \phi^i}{\partial x}\right] + m^i(t)\phi^i = 0, \quad t > t_0,\ x \in (0,1), \tag{1}$$

$$\left[v^i(t)\phi^i(t,x) - \sigma^i \frac{\partial \phi^i}{\partial x}\right]_{x=0} = F^i(t), \tag{2}$$

$$\left[-\sigma^i \frac{\partial \phi^i}{\partial x}\right]_{x=1} = 0, \tag{3}$$

$$\phi^i(t_0,x) = \hat{\phi}^i(x), \tag{4}$$

where the functions $\hat{\phi}^i(x)$ $(i = 1,2,\dots,s)$ are the initial distributions, and the σ^i are the diffusion coefficients, that allow to take into account the variability of development rate among individuals. The functions $F^i(t)$ represent the fluxes from a stage to the next one. More precisely, $F^1(t)$ is the egg production flux and it is given by:

$$F^1(t) = \int_0^1 a_0(T(t))\, f(x)\phi^s(t,x)\, dx \tag{5}$$

where $a_0(T(t))\, f(x)$ is the number of eggs produced per adult with physiological age in $(x, x+dx)$ per time unit, $a_0(T(t))$ takes into account the effect of time-dependent temperature $T(t)$ and $f(x)$ is the maximum age specific fertility profile. In our model, we include the influence of diapause. In particular, diapause depends on daylight D and on time t. Thus, equation (5) is modified as follows:

$$F^1(t) = \begin{cases} (1 - diap(D)) \int_0^1 a_0(T(t))\, f(x)\phi^s(t,x)\, dx & for\ t \in [t_{min}^{diap}, t_{max}^{diap}], D \le D_{max} \\ \int_0^1 a_0(T(t))\, f(x)\phi^s(t,x)\, dx + A_{diap} & the\ first\ t\ out\ of\ [t_{min}^{diap}, t_{max}^{diap}] \\ & when\ D \ge D_{min}, \bar{T}_{min} \ge T_d \\ \int_0^1 a_0(T(t))\, f(x)\phi^s(t,x)\, dx & otherwise \end{cases} \quad (6)$$

where $diap(D)$ is the percentage of eggs entering diapause (depending on daylight D), $\bar{T}_{min}$ is the average of the minimum temperature of the previous week, D_{max} is the maximum daylight under which the diapause is active, D_{min} is the minimum daylight over which the diapause end, t_{min}^{diap} is the initial time of diapause, t_{max}^{diap} is the final time of diapause, and A_{diap} is the number of diapausing eggs accumulated during the period in which diapause is active.

For $i > 1$, the fluxes from stage $i-1$ to stage i are given by

$$F^i(t) = v^{i-1}(t)\phi^{i-1}(t,1), \qquad i = 2, \dots, s. \quad (7)$$

The number of individuals in stage i at time t can be obtained integrating functions $\phi^i(t,x)$ over the physiological age:

$$N^i(t) = \int_0^1 \phi^i(t,x)dx. \quad (8)$$

In this model we assume that the host's availability and the availability of breeding sites are not limiting factors, then they do not affect the basic demographic processes (development, mortality, fecundity).

2.1. Biodemographic functions for Ae. albopictus

We assume the population of *Ae. albopictus* being composed by five stages: four immature stages (eggs, larvae, pupae, sexually immature adults), and an adult reproductive stage. For each stage, development and mortality rate functions are specified. Moreover, for the reproductive adult stage also the fecundity rate

function is stated. Fitted functions and literature data for biodemographic rate functions are reported in the Supplementary Materials.

2.1.1. Development rate function

Development times of *Ae. albopictus* are available in literature for eggs, larvae, pupae, and sexually immature adults: for the egg stage, data come from Delatte et al. (2009) and from Monteiro et al. (2007); for the larval and the pupal stages, data come from Delatte et al. (2009), Hien (1975), and Monteiro et al. (2007); for the sexually immature adults, data come from Calado and Navarro-Silva (2002), and Delatte et al. (2009).

For each developmental stage, we choose a function that well represent literature data. Egg development rate, is described by a third degree polynomial (see Kontodimas et al., 2004):

$$v^1(T(t)) = \begin{cases} aT^2\left(T_{sup} - T\right) & 0 \le T \le T_{sup} \\ 0 & otherwise \end{cases} \tag{9}$$

while, for the development rates of larvae, pupae and sexually immature adults we use the Brière function (Brière et al., 1999):

$$v^i(T(t)) = \begin{cases} aT\left(T - T_{inf}\right)\sqrt{T_{sup} - T} & T_{inf} \le T \le T_{sup} \\ 0 & otherwise \end{cases} \qquad i = 2,3,4\,. \tag{10}$$

The parameters a, T_{inf}, and T_{sup} in equations (9) and (10) are estimated using a least square estimation method (Table 1).

Table 1. Estimates of parameters in equations (9) and (10) for the pre-reproductive stages.

	a	T_{inf} (ºC)	T_{sup} (ºC)
Eggs	0.0000416657		37.3253
Larvae	0.00008604	8.2934	36.0729
Pupae	0.0003102	11.9433	40
Sexually immature adults	0.0001812	7.7804	35.2937

Data on the life-span of reproductive adults are not available in literature. Thus, the reproductive adult development rate function is obtained in a different way that involves the definition of the fecundity rate function (see the Subsection 2.1.3).

2.1.2. Mortality rate function

The mortality rate function is obtained from the average stage proportional mortality as function of temperature. Data on the proportion of dying individuals can be found in literature for eggs, larvae, and pupae. For these stages, the proportion of dying individuals can be described by a second order polynomial:

$$M^i(T(t)) = \begin{cases} p_1T^2 + p_2T + p_3 & T_{inf} \le T \le T_{sup} \\ p_1T_{inf}^2 + p_2T_{inf} + p_3 & T < T_{inf} \\ p_1T_{sup}^2 + p_2T_{sup} + p_3 & T > T_{sup} \end{cases} \qquad i = 1,2,3 \tag{11}$$

where T_{inf} and T_{sup} are the minimum and maximum temperatures so that $M^i(T)$ assumes a maximum value of 0.9.

Then, the mortality rate function is defined as follows (see Gilioli et al., 2016):

$$\mu^i(T(t)) = \begin{cases} -v^i(T(t))\log\left(1 - M^i(T(t))\right) & T_{inf}^{\mu} \le T \le T_{sup}^{\mu} \\ -v^i(T_{inf})\log\left(1 - M^i(T_{inf})\right)\left[a(T_{inf} - T)^2 + 1\right] & T < T_{inf}^{\mu} \\ -v^i(T_{sup})\log\left(1 - M^i(T_{sup})\right)\left[b(T - T_{sup}) + 1\right] & T > T_{sup}^{\mu} \end{cases} \qquad i = 1,2,3 \tag{12}$$

195 with the interval $\left[T_{inf}^{\mu}, T_{sup}^{\mu}\right]$ contained in the interval of positivity of the development rate function.
196 Parameters in function (11) are obtained by fitting literature data in Delatte et al. (2009) throughout a least
197 square method (Table 2).

198

199 **Table 2.** Parameters of the average stage proportional mortality (11) for eggs, larvae, and pupae.

	p_1	p_2	p_3	T_{inf} (°C)	T_{sup} (°C)
Eggs	0.002869	-0.1417	2.1673	11.72	37.69
Larvae	0.002793	-0.1255	1.5768	6.27	38.65
Pupae	0.003289	-0.1437	1.6197	5.77	37.93

200 Parameters a and b in function (12) are chosen to obtain the desired slope for low and high temperatures
201 assuring a well connection with the shape of the function μ^i in the interval $\left[T_{inf}^{\mu}, T_{sup}^{\mu}\right]$ (granting in the two
202 points T_{inf}^{μ} and T_{sup}^{μ} only the continuity of the function μ^i). Values of parameters a, b, T_{inf}^{μ}, T_{sup}^{μ} are
203 reported in Table 3.

204 **Table 3.** Parameters of the mortality rate functions (12).

	a	b	T_{inf}^{μ} (°C)	T_{sup}^{μ} (°C)
Eggs	0.05	0.018	12	30.5
Larvae	0.2	0.15	17	30.5
Pupae	0.1	0.2	17	37.5

205 Data on the proportion of dying adults are not available separately for sexually immature and reproductive
206 adults. Then the choice is to consider, for these two stages, the same mortality function that is assumed a
207 constant parameter to be estimated (see the Subsection 2.1.3).
208 We assume a density-dependent larval mortality described by the function:

$$m^2\big(T(t)\big) = \mu^2\big(T(t)\big)\big(1 + \alpha N^2(t)\big)^{\beta} \qquad (13)$$

obtained using a simple power function, where $N^2(t)$ is the number of larvae (stage 2) present in the system at time t, while α and β are two constant parameters to be estimated. The power function proposed for the density-dependence in the mortality rate is more flexible than the linear function used in Guzzetta et al. (2016b), and in Jia et al. (2016). For the other stages, we do not assume density-dependent mortality.

$$m^i(T) = \mu^i(T) \qquad i = 1,3,4,5.$$

2.1.3. Fecundity rate function and the reproductive adult stage

The fecundity function is assumed to be influenced only by temperature, that is reproductive females produce the same number of eggs independently of the physiological age. We choose a Brière function to describe the temperature-dependent fecundity rate of reproductive adults:

$$a_0(T(t))f(x) = \begin{cases} aT\big(T - T_{inf}\big)\sqrt{T_{sup} - T} & T_{inf} \le T \le T_{sup}\ , \quad 0 \le x \le 1 \\ 0 & otherwise \end{cases} \qquad (14)$$

Development, mortality and reproduction for adults are modeled together using data on fecundity and longevity reported by Delatte et al. (2009). Data on the duration of the oviposition period (Delatte et al. 2009), calculated for a survival of 1% (Table 4), allow to obtain the reproductive adult development rate which is approximately constant and equal to 0.015 *1/day*. Parameters of the fecundity rate function (14) are estimated (Table 5) using a nonlinear regression method to fit the total number of eggs laid by a female (Table 4, second row) at fixed temperatures. The simulated number of eggs laid by a female is obtained integrating (14) on the physiological age using the parameters in Table 5 and the constant development rate of 0.015 *1/day*. Results are reported in Table 4 (third row).

Table 4. First row: oviposition period considering a survival of 1%; second row: total number of eggs/female (Delatte et al., 2009); third row: simulated total number of eggs/female of *Ae. albopictus* at different temperatures.

	T=15 ºC	T=20 ºC	T=25 ºC	T=30 ºC	T=35 ºC
Oviposition period	65	63.11	64.46	75.83	30.17
Total number of eggs/female (Delatte et al., 2009)		60.39	150.8	195.04	20.2
Total number of eggs/female (simulated)		62.03	147.59	196.93	20.17

Table 5. Parameters of the fecundity rate functions (14) of *Ae. albopictus* obtained using a nonlinear regression method on the total number of eggs laid by a female. In parenthesis the SD of the estimates.

a	T_{inf} (ºC)	T_{sup} (ºC)
0.0032	16.24	35.02
(0.00012)	(0.3454)	(0.0085)

Given the selected development and fecundity rate functions, the mortality rate for the adults are estimated to well approximate the net reproductive rate reported by Delatte et al. (2009) using a least square method (Table 6). The value obtained for the adult mortality rate is 0.067 *1/day*, and it is used also as mortality rate for the sexually immature adult stage.

Table 6. Net reproductive rates of *Ae. albopictus* (Delatte et al., 2009) and simulated net reproductive rate (using an adult mortality of 0.067) at different temperatures.

	T=20 ºC	T=25 ºC	T=30 ºC	T=35 ºC
Net reproductive rate (Delatte et al., 2009)	11.05	33.08	43.29	0.04
Net reproductive rate (simulated)	13.56	32.26	43.05	4.32

2.2. Diapause

243 In our model, a certain percentage of mosquito eggs enters in diapause and survive to winter temperatures.
244 We assume this percentage depending on the daylight period, following the formula:

245 $$diap(D) = \frac{1}{1 + e^{3.04(D-12.62)}}$$

246 where D represents the daylight period in hours (Lacour et al., 2015).
247 To model diapause, a storage of eggs A_{diap} has been created starting from $t_{min}^{diap} = 1^{st}$ July up to $t_{max}^{diap} =$
248 31^{st} December, when daylight is less than or equal to $D_{max} = 15$ hours. Diapausing eggs are subject to
249 mortality. Fitting data on the surviving eggs after diapause reported in Thomas et al. (2012) we obtain the
250 following diapausing egg mortality rate:

251 $$m^{diap}(T) = 0.05301e^{-0.164} \quad .$$

252 As soon as the daylight is equal or greater than $D_{min} = 11.25$ hours and the average of the minimum
253 temperature of the previous week is equal or greater than $T_d = 12.5$ °C the survived eggs stored in A_{diap}
254 break the diapause state. Then, the eggs start again the development from physiological age 0 following the
255 rate function (9).

256 **3. Data**

257

258 To run the model, data on temperature and daylight duration are needed. Biodemographic functions of
259 adults are regulated by air temperature, while biodemographic functions of immature stages are driven by
260 5 cm depth water temperature.
261 Data on presence of mosquito eggs are available for some locations in Bolzano province. Hourly
262 temperature data for these locations were simulated on the basis of daily time series of maximum and
263 minimum air temperature (Tx, Tn) from nine weather stations located in Vipiteno, Bressanone, Brunico,
264 Bolzano and Salorno (Meteorological Service of the Autonomous Province of Bolzano), Rovereto, Mori-

265 Loppio, San Michele all'Adige and Aldeno (Meteotrentino). To generate hourly temperature data, we apply
266 the following algorithm:
267 1. For the observation sites the daily Tx, Tn for the average year (mean of the period 2000-2012) are rebuild
268 on the basis of Tx and Tn of the nine weather stations. To do it, a suitable geo-statistical procedure
269 consisting of weighted averages, with weight inversely proportional to squared distances is applied to the
270 data of the weather stations previously homogenized to the observation point for height and aspect by the
271 method described in section S1 of the Supplementary materials. The adopted weighting procedure makes
272 negligible the contribution of more remote stations;
273 2. Tx and Tn for each reference point are then adopted to simulate hourly air temperatures by means of the
274 de Wit's algorithm (de Wit et al., 1978);
275 3. A reference year with 8760 hourly values are obtained by averaging hourly values of the original period
276 2000-2012;
277 4. Hourly water temperatures at 5 cm of depth for the reference year are then obtained by means of a semi-
278 empirical model based on the Fourier equation of heat diffusion (Larnier et al., 2010) applied to hourly air
279 temperatures (see Supplementary material section S2).
280 Data on egg population dynamics were made available by the Agency for the Environment and Climate
281 Protection of the Bolzano Province (Italy), and used to calibrate the parameters of the density-dependent
282 larval mortality rate of *Ae. albopictus*. These data refer to the weekly mean abundance of eggs collected
283 from ovitraps deployed in seven locations (Brunico, Vipiteno, Appiano, Caldaro, Bressanone, Bolzano and
284 Laives) of the Bolzano Province in the reference period 2013-2015. A total number of 105 georeferenced
285 ovitraps were monitored in the area (6 in Brunico, 6 in Vipiteno, 9 in Appiano, 8 in Caldaro, 8 in
286 Bressanone, 53 in Bolzano and 15 in Laives). The egg population abundance in each site is expressed as
287 the mean number of eggs sampled per week in the reference period. Egg abundance is calculated
288 considering only samples with number of eggs greater than zero. Where samples are always zero, egg
289 abundance is set equal to zero and the site is considered outside the area of potential distribution. We
290 purposely chose sites in a wide altitudinal range to test model's capability to predict the presence, the

absence and eventually the abundance of mosquito eggs under varying meteorological regimes (Table 7). Since 2013, treatment and monitoring campaigns aimed at preventing the spread of *Ae. albopictus* have started in the Bolzano Province. Having not clear indications and data aimed at quantifying the potential role of treatments on the overall mosquito population distribution and abundance in the reference area it was not possible to include this aspect in the model. Therefore, we introduce the simplifying assumption that the effect of treatments on the overall mosquito population distribution and abundance was negligible.

Table 7. Geographic coordinates of the centroid of the area in which eggs are sampled, in the seven locations of the Bolzano Province. For each centroid is reported the altitude in *m* a.s.l..

Location	Latitude (°N)	Longitude (°E)	Altitude (*m*)	Mosquito Presence/absence
Brunico	46°47'16,29"	11°56'17,06"	830	Absent
Vipiteno	46°53'33,01"	11°26'00,66"	949	
Appiano	46°27'34,38"	11°15'00,46"	516	Present (population density ≤ 30 eggs/week)
Caldaro	46°24'31,77"	11°13'58,24"	530	
Bressanone	46°44'03,58"	11°38'29,23"	626	
Bolzano	46°30'26"	11°21'11"	290	Present (population density > 30 eggs/week)
Laives	46°26'15"	11°20'49"	250	

To obtain an estimate of α and β in (13), data on egg abundance in the different locations of the Bolzano province are used (Table 8). A procedure similar to that used for the sites of the Bolzano Province was also applied in order to rebuild meteorological data for the whole European area (grid with pixel 0.25 × 0.25 degrees lat - lon referred to a rectangular area ranging from 34° to 72° North and -11° to 42° East). In such case the daily time series 2000-2012 of Tx, Tn for each cell are produced by a suitable interpolation procedure (weighted average with weight inversely proportional to squared distances on data previously

306 homogenized for the height adopting a lapse rate of -0.5°C/100 m) applied to maximum and minimum
307 temperatures from synoptic meteorological stations beginning to the NOAA-GSOD dataset (National
308 Oceanic and Atmospheric Administration, National Climatic Data Centre, Global Summary Of the Day).
309 Also in this case hourly air temperatures (AT) are obtained by means of the de Wit algorithm (de Wit et al.,
310 1978) and hourly water temperatures are obtained by means of a semi-empirical model based on the Fourier
311 equation of heat diffusion (Larnier et al., 2010).

312

313 **4. Results**

314

315 *4.1. Model calibration*

316

317 The model is calibrated estimating the parameters of a density-dependent mortality rate function for the *Ae.*
318 *albopictus* larvae. To run the model an initial population of 100 adults at 1st of May, with physiological age
319 uniformly distributed between 0 and 1, is considered. Air temperature is used for simulating the population
320 abundance of the adult stage while water temperature at 5 cm depth is used for simulating the population
321 dynamics of the immature stages. A reference year of 8760 hourly values is obtained averaging hourly
322 values of the original period 2000-2012 as explained above.
323 Parameters α and β in formula (13) are estimated using a least square method in order to minimize the
324 difference between the simulated and the mean number of observed eggs per week in the different locations
325 of the Bolzano province. In particular, we solve the problem:

326 $$\min_{\alpha,\beta} \sum_{i=1}^{7} \left(\overline{N}_i^1(\alpha,\beta) - E_i\right)^2$$

327 where $\overline{N}_i^1(\alpha,\beta)$ is the mean number of eggs simulated in the location i, depending on the parameters α,β,
328 while E_i is the number of eggs collected in the same location.

329 The mean number of eggs in the simulation is obtained running the model for 20 years in order to obtain a
330 stable pattern of population dynamics and the yearly mean over the last year is used. In table 8 are reported
331 the results of model calibration. The model is able to predict the mean number of eggs in the locations
332 where the species is present. Where the mosquito is not established (Brunico and Vipiteno) the model
333 correctly predicted the absence of eggs. The values of the estimated parameters are $\alpha = 0.1606$, $\beta =$
334 0.5133, with 95% confidence intervals $[0.0145, 1.7787]$ and $[0.1179, 0.9087]$, respectively.

335

336 **Table 8.** Mean number of mosquito eggs in the different locations of the Bolzano Province. Only locations
337 in which the mosquito is present are here considered.

Location	Mean number of observed eggs/week	Estimated number of eggs
Appiano	13.96	26.77
Caldaro	21.38	18.20
Bressanone	2.05	5.08
Bolzano	80.77	72.07
Laives	112.63	115.46

338

339 *4.2. Maps of mosquito potential distribution, abundance and activity*

340

341 The calibrated model is used for deriving maps representing the area of potential distribution, abundance
342 and activity (expressed as number of weeks between the spring egg hatching and the beginning of autumn
343 egg diapause) of *Ae. albopictus* in each location of a 0.25 x 0.25° lat lon grid covering Europe. We run the
344 model for each point of the grid, using 100 adults at 1st of May, with physiological age uniformly distributed
345 between 0 and 1 as initial conditions. In each point, the simulation covers a 10 years period. An index of

mosquito population abundance is derived by calculating the mean number of adult females per area unit over the last year of simulation. This index is mapped for the simulated area in Fig. 1.

The model predicts an area of potential distribution that comprises the Iberian peninsula, most of France and Italy, the Balkan peninsula and large parts of Hungary, Romania and Ukraine. Isolated populations might be present in some areas of central Europe where climate is more favourable. The model predicts the presence of *Ae. albopictus* in central Germany and in southern Czech Republic in agreement to the latest detections reported in Kuhlisch et al. (2018) and Rudolf et al. (2018), respectively. The predicted population abundance shows a negative gradient from southern to northern Europe. The highest population abundance is predicted for the Mediterranean countries particularly in proximity of the coastal areas (especially in the Italian peninsula, southern Spain, southern Portugal and southern France).

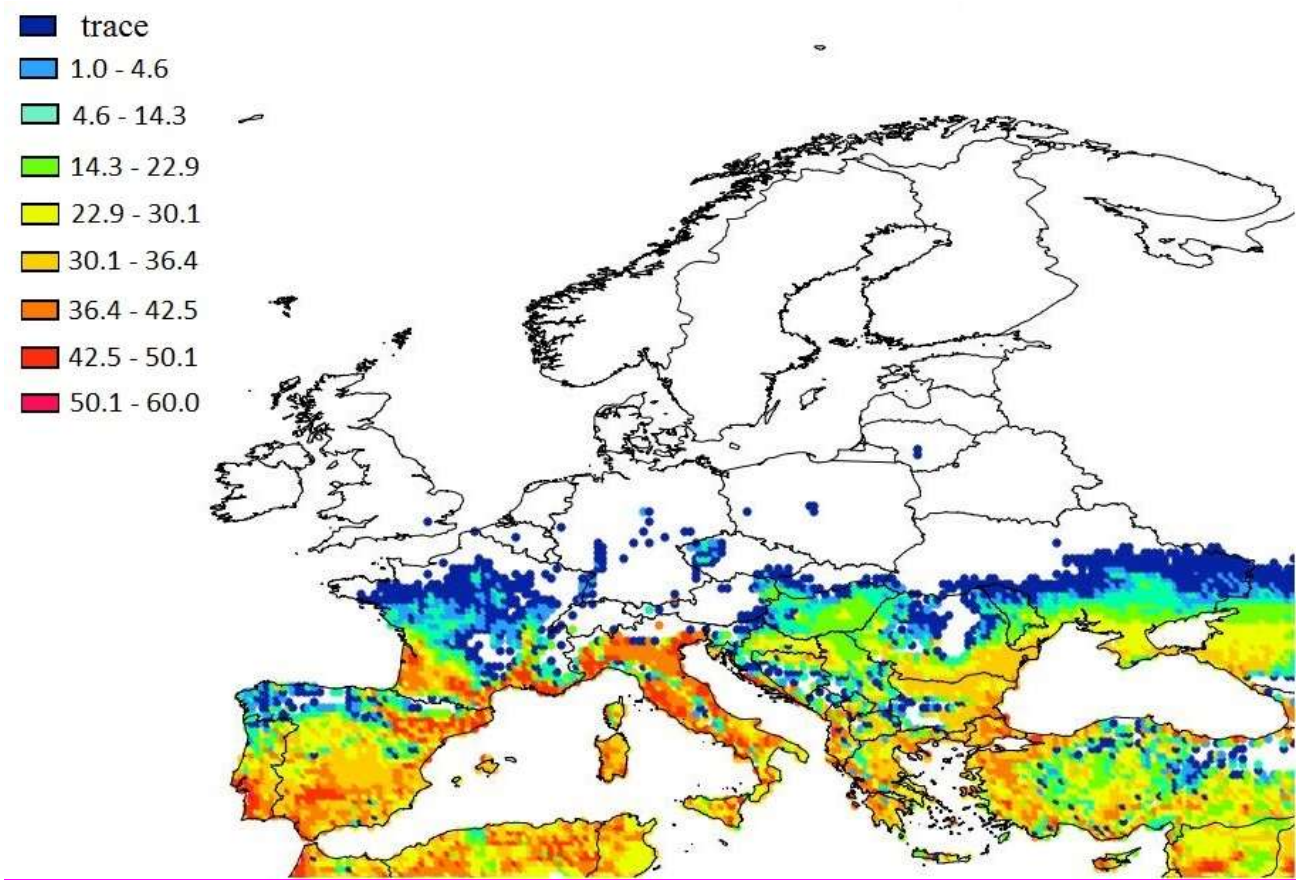

Figure 1. Heat map showing the simulated index of *Ae. albopictus* population abundance (mean number of adult females per area unit on the last year of simulation) in Europe. Temperature data used in the model

refer to the period 2000-2012. The dark blue colour class is defined as 'trace' and represents areas in which the abundance is positive and less than 1.

Another important aspect linked to the potential impact of a vector is represented by the seasonal activity period, i.e. the time between egg hatch and the beginning of diapause (Caminade et al., 2012; ECDC, 2009; Medlock et al., 2006). The outputs of the simulation are shown in Fig. 2. The highest population activity (up to 19 weeks) is found in southern Europe (especially in the south of Spain, Portugal, Greece, Italy, Cyprus, and Crete) mainly in the coastal areas. The seasonal activity decreases towards the northern distribution limit of the species with a less evident gradient respect to population abundance.

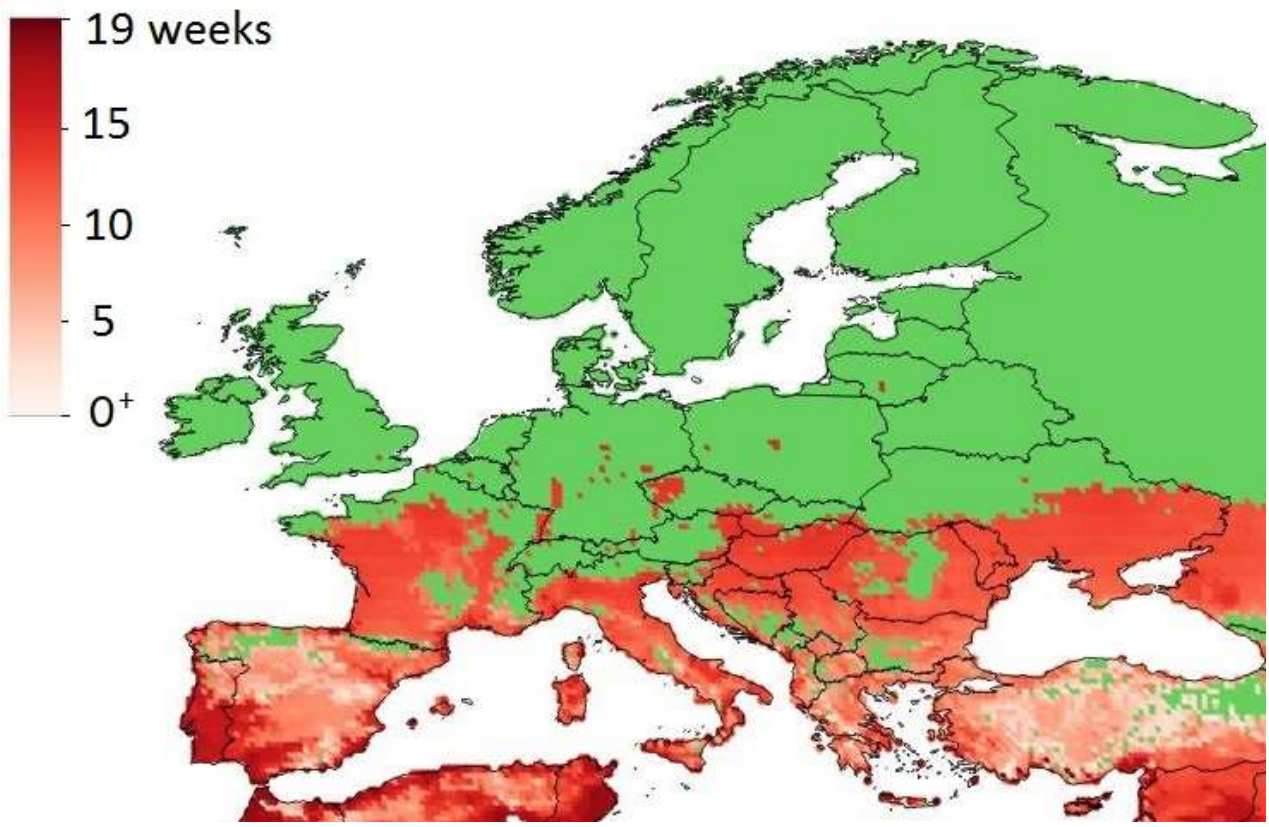

Figure 2. Simulated mosquito seasonal activity expressed as number of weeks between the spring egg hatching and the beginning of autumn egg diapause (pale pink to dark red colour gradient). The green colour refers to areas characterized by the absence of the species.

5. Discussions and conclusions

Since the first introduction in Europe, *Ae. albopictus* showed a rapid expansion of its area of establishment raising concerns related to potential vector-borne diseases outbreaks in Europe. Among other variables, temperature and precipitation patterns are major drivers in determining the habitat suitability of *Ae. albopictus*, while the duration of daylight is fundamental in triggering diapause and thus ensuring the survival towards the northern distribution limit. This work presents the results of a mechanistic model predicting the potential distribution of the species and evaluating the abundance and the seasonal period of activity as main factors in determining the impact of *Ae. albopictus* in Europe. The model aims at realistically represent the physiological and ecological responses of the species to its major abiotic drivers, specifically air temperature for adult stages, water temperature for immature stages, and both water temperature and duration of daylight for simulating diapause. Furthermore, we introduce a biotic controlling factor in terms of density-dependent mortality affecting larvae.

Overall, the simulated area of potential distribution and the northern limit comply with the most updated distribution reports of *Ae. albopictus* in Europe (ECDC and EFSA, 2019). The model is able to foresee the presence of the species in southern Europe where the favorable climate allowed its establishment. The interpretation of data related to the absence of the species must be carefully evaluated, since the mosquito has not reached the maximum potential distribution in Europe as clearly demonstrated by the absence in south-east part of the Iberian peninsula as well as many other parts of the Mediterranean basin characterized by a suitable climate. Although the species has not reached a stable distribution in central Europe, the current presence of the species in southern UK, Belgium, Germany, Switzerland, Austria, Czech Republic, Romania, Serbia, Bulgaria, Hungary and Slovakia (ECDC and EFSA, 2019) is correctly predicted by the model. Furthermore, the model predicts the presence of established populations in limited areas of Poland, Lithuania, Ukraine, Moldavia and Cyprus, thus these areas might be considered as potentially suitable for the introduction of the species. Unlike ECDC and EFSA (2019), the model does not predict the presence of mosquito populations in the Netherlands. However, the mosquito populations in this country are not

398 classified as established. Unlike some correlative models (Caminade et al., 2012; Proestos et al., 2015) the
399 simulated potential mosquito distribution does not reach northern Europe (e.g. the south and the west part
400 of the UK, Ireland, western Scotland and Denmark). In our model, the simulation of the diapause process
401 makes year-round survivorship of the species (i.e. establishment) relatively independent of the mild climatic
402 conditions found in coastal areas. This enables exploring the full potential geographic distribution of the
403 species, including areas that may be suitable but where correlative modeling approaches may predict
404 absence due to partial niche characterization in the underlying occurrence data (see Soberón and Nakamura,
405 2009).
406 A major output of our model is the quantification of the projected mosquito population abundance in
407 Europe. Our model shows a sharp latitudinal gradient in respect to *Ae. albopictus* population abundance.
408 Correlative models do not provide any information about population abundance and habitat suitability may
409 not be considered as a proxy of potential species abundance. However, the patterns of habitat suitability
410 projected by most correlative models show a positive east-west gradient with a clear Atlantic influence (i.e.,
411 the habitat suitability is positively influenced by the proximity of the Atlantic ocean as noticed in Portugal)
412 (Benedict et al., 2007; Caminade et al., 2012; Fischer et al., 2014; Proestos et al., 2015). Erguler et al.
413 (2016) provided a mosquito habitat suitability index based on the ratio between the predicted population
414 size in a certain location and the minimum population size allowing the establishment of *Ae. albopictus*. In
415 accordance to our model, high population abundance is expected in southern and western Spain and
416 Portugal, southern France, the coastal areas of Italy and the coastal areas of Bulgaria and Romania. In
417 contrast to Erguler et al. (2016) our model projections do not allow the establishment of *Ae. albopictus*
418 above the 50th North parallel. Especially, in accordance with the most updated *Ae. albopictus* distribution
419 maps (ECDC, 2019), our model does not allow the establishment of populations in the UK (with the
420 exception of a single point in southern London) and in Ireland.
421 Another important factor in the determining the risks linked to vector-borne diseases is the mosquito
422 seasonal activity period (Caminade et al., 2012; ECDC, 2009; Medlock et al., 2006). In our model, the
423 activity pattern shows a less evident south-north latitudinal gradient if compared with the predicted

424 abundance. This might be caused by the influence of the daylight length (higher in northern Europe if
425 compared to southern Europe) which prevents a fast decrease of the activity period along the south-north
426 latitudinal gradient.
427 The pattern of activity predicted in our model differs from the pattern presented in ECDC (2009) and in
428 Caminade et al. (2012) where the east-west gradient is still prominent as well as a Mediterranean influence
429 (i.e. the positive influence on population activity in proximity of the Mediterranean Sea).
430 Our model does not take into account the potential role of rainfall on physiological and ecological responses
431 of the investigated species. However, given the fact that *Ae. albopictus* is able to produce eggs in any type
432 of natural and/or human-made water body, this shortcoming does not have strong impact on the mosquito
433 pattern of establishment at the large-scale. However, population abundance might be influenced by the land
434 use, in particular in relation to the availability of water at local and meso-scale.
435 The reliability of any quantitative risk projection is related to the possibility of calibrating and validating
436 model outputs, particularly if data are collected in the area where the risk is assessed. Our model is
437 calibrated in the capacity to foresee the establishment along an altitudinal gradient up to an altitude that
438 prevents population survival in winter. Model calibration also allows to produce realistic projections of
439 population abundance in terms of number of eggs per area unit, considering both the influence of climate
440 and density-dependent regulation. Calibrating the model using the eggs is of paramount importance, since
441 the sampling of this stage produces the most reliable estimation of population abundance. The model
442 presented in this paper might be a suitable tool for the development of knowledge-based strategies aimed
443 at the management of *Ae. albopictus* and for the implementation of effective control measures against
444 vector-borne diseases. The projection of seasonal activity period and mosquito population abundance might
445 be used in combination with epidemiological models in order to produce risk maps of vector-borne diseases
446 outbreaks in Europe at different levels of resolution (from local to continental level). At continental level,
447 the model might support the identification of suitable areas in Europe where *Ae. albopictus* has not yet been
448 found in order to prevent the introduction in new areas. The maps on potential distribution together with
449 maps on expected population abundance can be used to develop surveillance programs targeting vector

450 populations or prioritize area for vector control that are at higher risk of vector-borne diseases outbreaks.
451 The model might be used to support the design and the implementation of precision target control activities
452 against *Ae. albopictus*. This requires the integration of the simulation model within a decision support tool
453 in which GIS technology allows the management of environmental information strata and model outputs at
454 high resolution (Rossi et al., submitted). Normally these systems are suited for supporting pest control
455 activities at limited spatial extensions with high spatial and temporal resolution data on water and air
456 temperature, relative humidity, cloudiness, breeding sites presence, size and distribution etc. At micro-
457 scale it is also possible to describe the effects of environmental alteration due to human activities (e.g. effect
458 of thermal pollution due to industrial effluents, change in the land use) on mosquito population
459 abundance.The model could also aid in assessing those mosquito control strategies based on the induction
460 of sterility such as the conventional SIT or by the exploitation of the endosymbiont bacterium Wolbachia
461 that can induce both sterility (Bourtzis et al., 2104; Calvitti et al., 2012; Moretti et al., 2018a; see e.g.,
462 Gutierrez et al., 2019 for how the impact of sterility could be assessed) and virus protection (Moretti et al.,
463 2018b).
464 Future model developments will focus on the introduction of scenarios related to the effects of: i) control
465 measures, ii) water availability and iii) climate change, on the overall mosquito population distribution,
466 activity and abundance.

467 **Acknowledgements**

468 We thank the Agency for the Environment and Climate Protection of the Bolzano Province for providing
469 datasets related to *Ae. albopictus* egg population.

470

471 **References**

472 Adhami, J., & Reiter, P. (1998). Introduction and establishment of *Aedes* (Stegomyia) *albopictus* skuse (Diptera:
473 Culicidae) in Albania. *Journal of the American Mosquito Control Association*, *14*(3), 340-343.

474 Angelini, R., Finarelli, A., Angelini, P., Po, C., Petropulacos, K., Macini, P., Fiorentini, C., Fortuna, C., Venturi, G.,
475 Romi, R., Majori, G., Nicoletti, L., Rezza, G., & Cassone, A. (2007). An outbreak of chikungunya fever in the province
476 of Ravenna, Italy. *Weekly releases (1997–2007)*, *12*(36), 3260.

477 Benedict, M. Q., Levine, R. S., Hawley, W. A., & Lounibos, L. P. (2007). Spread of the tiger: global risk of invasion
478 by the mosquito *Aedes albopictus*. *Vector-borne and zoonotic Diseases*, *7*(1), 76-85.

479 Bourtzis, K., Dobson, S. L., Xi, Z., Rasgon, J. L., Calvitti, M., Moreira, L. A., Bossin, H. C., Moretti, R., Baton, L.
480 A., Hughes, G.L., Mavingui, P., & Gilles, J. R. L. (2014). Harnessing mosquito–*Wolbachia* symbiosis for vector and
481 disease control. *Acta tropica*, *132*, S150-S163.

482 Brady, O. J., Johansson, M. A., Guerra, C. A., Bhatt, S., Golding, N., Pigott, D. M., Delatte, H., Grech, M. G.,
483 Leisnham, P. T., Maciel-de-Freitas, R., Styer, L. M., Smith, D. L., Scott, T. W., Gething, P. W., & Hay, S. I. (2013).
484 Modelling adult *Aedes aegypti* and *Aedes albopictus* survival at different temperatures in laboratory and field
485 settings. *Parasites & vectors*, *6*(1), 351.

486 Brady, O. J., Golding, N., Pigott, D. M., Kraemer, M. U. G., Messina, J. P., Reiner Jr, R. C., Scott, T. W., Smith, D.
487 L., Gething, P. W., & Hay, S. I. (2014). Global temperature constraints on *Aedes aegypti* and *Ae. albopictus*
488 persistence and competence for dengue virus transmission. *Parasites & vectors*, *7*(1), 338.

489 Brière, J. F., Pracros, P., Le Roux, A. Y., & Pierre, J. S. (1999). A novel rate model of temperature-dependent
490 development for arthropods. *Environmental Entomology*, *28*(1), 22-29.

491 Buffoni, G., & Pasquali, S. (2007). Structured population dynamics: continuous size and discontinuous stage
492 structures. *Journal of mathematical biology*, *54*(4), 555-595.

493 Calado, D. C., & Navarro-Silva, M. A. (2002). Influência da temperatura sobre a longevidade, fecundidade e atividade
494 hematofágica de *Aedes* (Stegomyia) *albopictus* Skuse, 1894 (Diptera, Culicidae) sob condições de laboratório. *Revista*
495 *Brasileira de Entomologia*, *46*(1), 93-98.

496 Calvitti, M., Moretti, R., Skidmore, A. R., & Dobson, S. L. (2012). *Wolbachia* strain w Pip yields a pattern of
497 cytoplasmic incompatibility enhancing a *Wolbachia*-based suppression strategy against the disease vector *Aedes*
498 *albopictus*. *Parasites & vectors*, *5*(1), 254.

499 Caminade, C., Medlock, J. M., Ducheyne, E., McIntyre, K. M., Leach, S., Baylis, M., & Morse, A. P. (2012).
500 Suitability of European climate for the Asian tiger mosquito *Aedes albopictus*: recent trends and future
501 scenarios. *Journal of the Royal Society Interface*, *9*(75), 2708-2717.

502 Campbell, L. P., Luther, C., Moo-Llanes, D., Ramsey, J. M., Danis-Lozano, R., & Peterson, A. T. (2015). Climate
503 change influences on global distributions of dengue and chikungunya virus vectors. *Philosophical Transactions of the*
504 *Royal Society B: Biological Sciences*, *370*(1665), 20140135.

505 Couto-Lima, D., Madec, Y., Bersot, M. I., Campos, S. S., de Albuquerque Motta, M., dos Santos, F. B., Vazeille, M.,
506 da Costa Vasconcelos, P. F., Lourenço-de-Oliveira, R., & Failloux, A.-B. (2017). Potential risk of re-emergence of
507 urban transmission of Yellow Fever virus in Brazil facilitated by competent *Aedes* populations. *Scientific reports*, *7*(1),
508 4848.

509 Delatte, H., Gimonneau, G., Triboire, A., & Fontenille, D. (2009). Influence of temperature on immature development,
510 survival, longevity, fecundity, and gonotrophic cycles of *Aedes albopictus*, vector of chikungunya and dengue in the
511 Indian Ocean. *Journal of medical entomology*, *46*(1), 33-41.

512 de Wit, C. T., Goudriaan, J., van Laar, H. H., Penning de Vries, F. W., Rabbinge R., van Keulen, H., Louwerse, W.,
513 Sibma, L., & de Jonge, C. (1978). Simulation of assimilation, respiration and transpiration of crops. *Simulation*
514 *Monographs*. Pudoc, Wageningen, The Netherlands, p. 140.

515 Ding, F., Fu, J., Jiang, D., Hao, M., & Lin, G. (2018). Mapping the spatial distribution of *Aedes aegypti* and *Aedes*
516 *albopictus*. *Acta tropica*, *178*, 155-162.

517 ECDC, 2009 Development of *Aedes albopictus* Risk Maps, Technical Report 0905. Available online:
518 http://ecdc.europa.eu/en/publications/Publications/0905_TER_Development_of_Aedes_Albopictus_Risk_Maps.pdf
519 (accessed 10 April 2019).

520 ECDC and EFSA, 2019. Mosquito maps. Available online: https://ecdc.europa.eu/en/disease-vectors/surveillance-
521 and-disease-data/mosquito-maps (accessed 10 April 2019).

522 Erguler, K., Smith-Unna, S. E., Waldock, J., Proestos, Y., Christophides, G. K., Lelieveld, J., & Parham, P. E. (2016).
523 Large-scale modelling of the environmentally-driven population dynamics of temperate *Aedes albopictus*
524 (Skuse). *PLoS One*, *11*(2), e0149282.

525 Erguler, K., Chandra, N. L., Proestos, Y., Lelieveld, J., Christophides, G. K., & Parham, P. E. (2017). A large-scale
526 stochastic spatiotemporal model for *Aedes albopictus*-borne chikungunya epidemiology. *PloS one*, *12*(3), e0174293.

527 Erickson, R. A., Presley, S. M., Allen, L. J., Long, K. R., & Cox, S. B. (2010). A stage-structured, *Aedes albopictus*
528 population model. *Ecological Modelling*, *221*(9), 1273-1282.

529 Erickson, R. A., Hayhoe, K., Presley, S. M., Allen, L. J., Long, K. R., & Cox, S. B. (2012). Potential impacts of
530 climate change on the ecology of dengue and its mosquito vector the Asian tiger mosquito (*Aedes albopictus*).
531 *Environmental Research Letters*, *7*, 034003 (6pp).

532 Fischer, D., Thomas, S. M., Neteler, M. G., Tjaden, N., & Beierkuhnlein, C. (2014). Climatic suitability of *Aedes*
533 *albopictus* in Europe referring to climate change projections: comparison of mechanistic and correlative niche
534 modelling approaches. *Eurosurveillance, 19*(6).

535 Gilioli, G., Pasquali, S., Parisi, S., & Winter, S. (2014). Modelling the potential distribution of *Bemisia tabaci* in
536 Europe in light of the climate change scenario. *Pest management science*, *70*(10), 1611-1623.

537 Gilioli, G., Pasquali, S., Ponti, L., Calvitti, M., Moretti, R., & Gutierrez, A. P. (2015) Modelling the potential
538 distribution and abundance of *Aedes albopictus* in Europe in light of the climate change scenario. *Conference: Impacts*
539 *of Environmental Changes on Infecious Diseases*, 23-25 March 2015, Sitges, Spain.

540 Gilioli, G., Pasquali, S., & Marchesini, E. (2016). A modelling framework for pest population dynamics and
541 management: An application to the grape berry moth. *Ecological modelling*, *320*, 348-357.

542 Gilioli, G., Pasquali, S., Martín, P. R., Carlsson, N., & Mariani, L., (2017a). A temperature-dependent physiologically
543 based model for the invasive apple snail *Pomacea canaliculata*. *International Journal of Biometeorology, 61*(11),
544 1899-1911.

Gilioli, G., Schrader, G., Grégoire, J. C., MacLeod, A., Mosbach-Schulz, O., Rafoss, T., Rossi, V., Urek, G., & van der Werf, W. (2017b). The EFSA quantitative approach to pest risk assessment–methodological aspects and case studies. *EPPO Bulletin*, *47*(2), 213-219.

Gilioli, G., Schrader, G., Carlsson, N., van Donk, E., van Leeuwen, C. H. A., Martín, P. R., Pasquali, S., Vilà, M., & Vos, S. (2017c). Environmental risk assessment for invasive alien species: A case study of apple snails affecting ecosystem services in Europe. *Environmental Impact Assessment Review*, *65*, 1-11.

Gjenero-Margan, I., Aleraj, B., Krajcar, D., Lesnikar, V., Klobučar, A., Pem-Novosel, I., Kurečić-Filipović, S., Komparak, S., Martić, R., Đuričić, S., Betica-Radić, L., Okmadžić, J., Vilibić-Čavlek, T., Babić-Erceg, A., Turković, B., Avšić-Županc, T., Radić, I., Ljubić, M., Šarac, K., Benić, N., & Mlinarić-Galinović, G. (2011). Autochthonous dengue fever in Croatia, August–September 2010. *Eurosurveillance*, *16*(9), 19805.

Gratz, N. G. (2004). Critical review of the vector status of *Aedes albopictus*. *Medical and veterinary entomology*, *18*(3), 215-227.

Guo, X. X., Zhu, X. J., Li, C. X., Dong, Y. D., Zhang, Y. M., Xing, D., Xue, R. D., Qin, C. F., & Zhao, T. Y. (2013). Vector competence of *Aedes albopictus* and *Aedes aegypti* (Diptera: Culicidae) for DEN2-43 and New Guinea C virus strains of dengue 2 virus. *Acta tropica*, *128*(3), 566-570.

Gutierrez, A. P. (1996). Applied population ecology: a supply-demand approach. *John Wiley & Sons*. New York, USA.

Gutierrez, A. P., & Ponti, L. (2013). Eradication of invasive species: why the biology matters. *Environmental entomology*, *42*(3), 395-411.

Gutierrez, A. P., Ponti, L., & Arias, P. A. (2019). Deconstructing the eradication of new world screwworm in North America: retrospective analysis and climate warming effects. *Medical and veterinary entomology*.

Guzzetta, G., Poletti, P., Montarsi, F., Baldacchino, F., Capelli, G., Rizzoli, A., Rosà, R., & Merler, S. (2016a). Assessing the potential risk of Zika virus epidemics in temperate areas with established *Aedes albopictus* populations. *Eurosurveillance*, *21*(15), 30199.

569 Guzzetta, G., Montarsi, F., Baldacchino, F. A., Metz, M., Capelli, G., Rizzoli, A., Pugliese, A., Rosà, R., Poletti, P.,
570 & Merler, S. (2016b). Potential risk of dengue and chikungunya outbreaks in northern Italy based on a population
571 model of *Aedes albopictus* (Diptera: Culicidae). *PLoS neglected tropical diseases*, *10*(6), e0004762.

572 Hien, D. S. (1975). Biology of *Aedes aegypti* (L., 1762) and *Aedes albopictus* (Skuse, 1895) (Diptera, Culicidae). III.
573 Effect of certain environmental conditions on the development of larvae and pupae. *Acta parasitologica polonica*, 23,
574 553–568.

575 Jia, P., Lu, L., Chen, X., Chen, J., Guo, L., Yu, X., & Liu, Q. (2016). A climate-driven mechanistic population model
576 of *Aedes albopictus* with diapause. *Parasites & vectors*, *9*(1), 175.

577 Jia, P., Chen, X., Chen, J., Lu, L., Liu, Q., & Tan, X. (2017). How does the dengue vector mosquito *Aedes albopictus*
578 respond to global warming?. *Parasites & vectors*, *10*(1), 140.

579 Knudsen, A. B. (1995). Global distribution and continuing spread of *Aedes albopictus*. *Parassitologia*, *37*(2-3), 91-
580 97.

581 Kobayashi, M., Nihei, N., & Kurihara, T. (2002). Analysis of northern distribution of *Aedes albopictus* (Diptera:
582 Culicidae) in Japan by geographical information system. *Journal of Medical Entomology*, *39*(1), 4-11.

583 Kontodimas, D. C., Eliopoulos, P. A., Stathas, G. J., & Economou, L. P. (2004). Comparative temperature-dependent
584 development of *Nephus includens* (Kirsch) and *Nephus bisignatus* (Boheman) (Coleoptera: Coccinellidae) preying on
585 *Planococcus citri* (Risso) (Homoptera: Pseudococcidae): evaluation of a linear and various nonlinear models using
586 specific criteria. *Environmental Entomology*, *33*(1), 1-11.

587 Kraemer, M. U. G., Sinka, M. E., Duda, K. A., Mylne, A. Q., Shearer, F. M., Barker, C. M., Moore, C. G., Carvalho,
588 R. G., Coelho, G. E., Van Bortel, V., Hendrickx, G., Schaffner, F., Elyazar, I. R. F., Teng, H.-J., Brady, O. J., Messina,
589 J. P., Pigott, D. M., Scot, T. W., Smith D. L., Wint G. R. W., Golding, N., & Hay, S. I. (2015). The global distribution
590 of the arbovirus vectors *Aedes aegypti* and *Ae. albopictus*. *elife*, *4*, e08347.

591 Kraemer, M. U. G., Reiner, R. C., Brady, O. J., Messina, J. P., Gilbert, M., Pigott, D. M., Yi, D., Johnson, K., Earl,
592 L., Marczak, L. B., Shirude, S., Weaver, N. D., Bisanzio, D., Perkins, T. A., Lai, S., Lu, X., Jones, P., Coelho, G. E.,
593 Carvalho, R. G., Van Bortel, W., Marsboom, C., Hendrickx, G., Schaffner, F., Moore, C. G., Nax, H. H., Bengtsson,

L., Wetter, E., Tatem, A. J., Brownstein, J. S., Smith, D. L., Lambrechts, L., Cauchemez, S., Linard, C., Faria, N. R., Pybus, O, G., Scott, T. W., Liu, Q., Yu, H., Wint, G. R. W., Hay, S. I., & Golding, N. (2019). Past and future spread of the arbovirus vectors *Aedes aegypti* and *Aedes albopictus*. *Nature microbiology*, *4*(5), 854.

Kuhlisch, C., Kampen, H., & Walther, D. (2018). The Asian tiger mosquito *Aedes albopictus* (Diptera: Culicidae) in Central Germany: Surveillance in its northernmost distribution area. *Acta tropica*, *188*, 78-85.

Lacour, G., Chanaud, L., L'Ambert, G., & Hance, T. (2015). Seasonal synchronization of diapause phases in *Aedes albopictus* (Diptera: Culicidae). *PloS one*, *10*(12), e0145311.

Lanzarone, E., Pasquali, S., Gilioli, G., & Marchesini, E. (2017). A Bayesian estimation approach for the mortality in a stage-structured demographic model. *Journal of mathematical biology*, *75*(3), 759-779.

Larnier, K., Roux, H., Dartus, D., & Croze, O. (2010). Water temperature modeling in the Garonne River (France). *Knowledge and Management of Aquatic Ecosystems*, (398), 04.

La Ruche, G., Souarès, Y., Armengaud, A., Peloux-Petiot, F., Delaunay, P., Desprès, P., Lenglet, A., Jourdain, F., Leparc-Goffart, I., Charlet, F., Ollier, L., Mantey, K., Mollet, T., Fournier, J. P., Torrents, R., Leitmeyer, K., Hilairet, P., Zeller, H., Van Bortel, W., Dejour-Salamanca, D., Grandadam, M., & Gastellu-Etchegorry, M. (2010). First two autochthonous dengue virus infections in metropolitan France, September 2010. *Eurosurveillance*, *15*(39), 19676.

Leta, S., Beyene, T. J., De Clercq, E. M., Amenu, K., Kraemer, M. U., & Revie, C. W. (2018). Global risk mapping for major diseases transmitted by *Aedes aegypti* and *Aedes albopictus*. *International Journal of Infectious Diseases*, *67*, 25-35.

Manica, M., Guzzetta, G., Poletti, P., Filipponi, F., Solimini, A., Caputo, B., Rosà, R., & Merler, S. (2017). Transmission dynamics of the ongoing chikungunya outbreak in Central Italy: from coastal areas to the metropolitan city of Rome, summer 2017. *Eurosurveillance*, *22*(44).

Medlock, J. M., Avenell, D., Barrass, I., & Leach, S. (2006). Analysis of the potential for survival and seasonal activity of *Aedes albopictus* (Diptera: Culicidae) in the United Kingdom. *Journal of Vector Ecology*, *31*(2), 292-305.

617 Medlock, J. M., Hansford, K. M., Schaffner, F., Versteirt, V., Hendrickx, G., Zeller, H., & Bortel, W. V. (2012). A
618 review of the invasive mosquitoes in Europe: ecology, public health risks, and control options. *Vector-borne and*
619 *zoonotic diseases*, *12*(6), 435-447.

620 Metelmann, S., Caminade, C., Jones, A. E., Medlock, J. M., Baylis, M., & Morse, A. P. (2019). The UK's suitability
621 for *Aedes albopictus* in current and future climates. *Journal of the Royal Society Interface*, *16*(152), 20180761.

622 Monteiro, L. C., de Souza, J. R., & de Albuquerque, C. M. (2007). Eclosion rate, development and survivorship of
623 *Aedes albopictus* (Skuse) (Diptera: Culicidae) under different water temperatures. *Neotropical entomology*, *36*(6),
624 966-971.

625 Moore, C. G., & Mitchell, C. J. (1997). *Aedes albopictus* in the United States: ten-year presence and public health
626 implications. *Emerging infectious diseases*, *3*(3), 329.

627 Mordecai, E. A., Cohen, J. M., Evans, M. V., Gudapati, P., Johnson, L. R., Lippi, C. A., Miazgowicz, K., Murdock,
628 C. C., Rohr, J. R., Ryan, S. J., Savage, V., Shocket, M. S., Ibarra, A. S., Thomas, M. B., & Weikel, D. P. (2017).
629 Detecting the impact of temperature on transmission of Zika, dengue, and chikungunya using mechanistic
630 models. *PLoS neglected tropical diseases*, *11*(4), e0005568.

631 Moretti, R., Marzo, G. A., Lampazzi, E., & Calvitti, M. (2018a). Cytoplasmic incompatibility management to support
632 Incompatible Insect Technique against *Aedes albopictus*. *Parasites & vectors*, *11*(2), 649.

633 Moretti, R., Yen, P. S., Houé, V., Lampazzi, E., Desiderio, A., Failloux, A. B., & Calvitti, M. (2018b). Combining
634 *Wolbachia*-induced sterility and virus protection to fight *Aedes albopictus*-borne viruses. *PLoS neglected tropical*
635 *diseases*, *12*(7), e0006626.

636 Pasquali, S., Soresina, C., & Gilioli, G. (2019). The effects of fecundity, mortality and distribution of the initial
637 condition in phenological models. *Ecological Modelling*, in press.

638 Paupy, C., Delatte, H., Bagny, L., Corbel, V., & Fontenille, D. (2009). *Aedes albopictus*, an arbovirus vector: from
639 the darkness to the light. *Microbes and Infection*, *11*(14-15), 1177-1185.

640 Petrić, M., Lalić, B., Ducheyne, E., Djurdjević, V., & Petrić, D. (2017). Modelling the regional impact of climate
641 change on the suitability of the establishment of the Asian tiger mosquito (*Aedes albopictus*) in Serbia. *Climatic*
642 *Change*, *142*(3-4), 361-374.

643 Poletti, P., Messeri, G., Ajelli, M., Vallorani, R., Rizzo, C., & Merler, S. (2011). Transmission potential of
644 chikungunya virus and control measures: the case of Italy. *PLoS One*, *6*(5), e18860.

645 Proestos, Y., Christophides, G. K., Ergüler, K., Tanarhte, M., Waldock, J., & Lelieveld, J. (2015). Present and future
646 projections of habitat suitability of the Asian tiger mosquito, a vector of viral pathogens, from global climate
647 simulation. *Philosophical Transactions of the Royal Society B: Biological Sciences*, *370*(1665), 20130554.

648 Reiter, P. (1998). *Aedes albopictus* and the world trade in used tires, 1988-1995: the shape of things to come?. *Journal*
649 *of the American Mosquito Control Association*, *14*(1), 83-94.

650 Reiter, P., & Sprenger, D. (1987). The used tire trade: a mechanism for the worldwide dispersal of container breeding
651 mosquitoes. Journal of the American Mosquito Control Association, 3, 494–501.

652 Rossi, V., Sperandio, G., Caffi, T., Simonetto, A., & Gilioli, G. (submitted). Critical success factors for the adoption
653 of Decision Tools in IPM. Agronomy.

654 Rudolf, I., Blažejová, H., Straková, P., Šebesta, O., Peško, J., Mendel, J., Šikutová, S., Hubálek, Z., Kampen, H., &
655 Schaffner, F. (2018). The invasive Asian tiger mosquito *Aedes albopictus* (Diptera: Culicidae) in the Czech Republic:
656 Repetitive introduction events highlight the need for extended entomological surveillance. *Acta tropica*, *185*, 239-
657 241.

658 Sallam, M., Fizer, C., Pilant, A., & Whung, P. Y. (2017). Systematic review: Land cover, meteorological, and
659 socioeconomic determinants of *Aedes* mosquito habitat for risk mapping. *International journal of environmental*
660 *research and public health*, *14*(10), 1230.

661 Santos, J., & Meneses, B. M. (2017). An integrated approach for the assessment of the *Aedes aegypti* and *Aedes*
662 *albopictus* global spatial distribution, and determination of the zones susceptible to the development of Zika
663 virus. *Acta tropica*, *168*, 80-90.

664 Sanz-Aguilar, A., Rosselló, R., Bengoa, M., Ruiz-Pérez, M., González-Calleja, M., Barceló, C., Borrás, D., Paredes-
665 Esquivel, C., Miranda, M. A., & Tavecchia, G. (2018). Water associated with residential areas and tourist resorts is
666 the key predictor of Asian tiger mosquito presence on a Mediterranean island. *Medical and veterinary*
667 *entomology*, *32*(4), 443-450.

668 Shragai, T., Tesla, B., Murdock, C., & Harrington, L. C. (2017). Zika and chikungunya: mosquito-borne viruses in a
669 changing world. *Annals of the New York Academy of Sciences*, *1399*(1), 61-77.

670 Soberón, J., & Nakamura, M. (2009). Niches and distributional areas: concepts, methods, and
671 assumptions. *Proceedings of the National Academy of Sciences*, *106*(Supplement 2), 19644-19650.

672 Soberón, J., & Peterson, A. T. (2011). Ecological niche shifts and environmental space anisotropy: a cautionary note.
673 *Revista Mexicana de Biodiversidad*, 82, 1348-1355.

674 Stanaway, J. D., Shepard, D. S., Undurraga, E. A., Halasa, Y. A., Coffeng, L. E., Brady, O. J., Hay, S. I., Bedi, N.,
675 Bensenor, I. M., Castañeda-Orjuela, C. A., Chuang, T.-W., Gibney, K. B., Memish, M. A., Rafay, A., Ukwaja, K. N.,
676 Yonemoto, N., Murray, C. J. L. (2016). The global burden of dengue: an analysis from the Global Burden of Disease
677 Study 2013. *The Lancet infectious diseases*, *16*(6), 712-723.

678 Thomas, S. M., Obermayr, U., Fischer, D., Kreyling, J., & Beierkuhnlein, C. (2012). Low-temperature threshold for
679 egg survival of a post-diapause and non-diapause European aedine strain, *Aedes albopictus* (Diptera:
680 Culicidae). *Parasites & vectors*, *5*(1), 100.

681 Trájer, A. J., Bede-Fazekas, Á., Bobvos, J., & Páldy, A. (2014). Seasonality and geographical occurrence of West
682 Nile fever and distribution of Asian tiger mosquito. *Időjárás/Quarterly Journal of the Hungarian Meteorological*
683 *Service*, *118*(1), 19-40.

684 Tran, A., L'Ambert, G., Lacour, G., Benoît, R., Demarchi, M., Cros, M., Cailly, P., Aubry-Kientz, M., Balenghein,
685 T., & Ezanno, P. (2013). A rainfall-and temperature-driven abundance model for *Aedes albopictus*
686 populations. *International journal of environmental research and public health*, *10*(5), 1698-1719.

687 Zheng, B., Yu, J., Xi, Z., & Tang, M. (2018). The annual abundance of dengue and Zika vector *Aedes albopictus* and
688 its stubbornness to suppression. *Ecological Modelling*, *387*, 38-48.

SUPPLEMENTARY MATERIALS

BIODEMOGRAPHIC FUNCTIONS FOR *Aedes albopictus*

- Development rate for immature stages. Continuous lines: development rate in formula (9) for eggs and development rate in formula (10) for the other immature stages. Asterisks: literature data for development rate (see Section 2.1.1 for references on data).

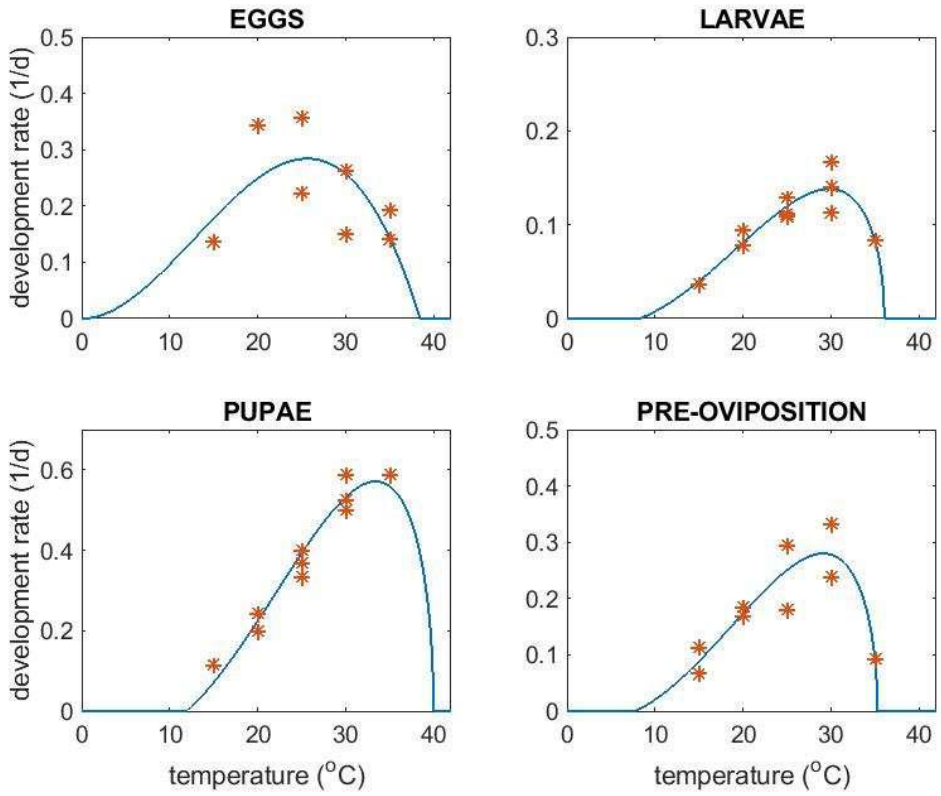

- Mortality rate for immature stages
  - Proportion of dying individuals for immature stages. Continuous line: formula (11). Asterisks: literature data (see Section 2.1.2 for references on data).

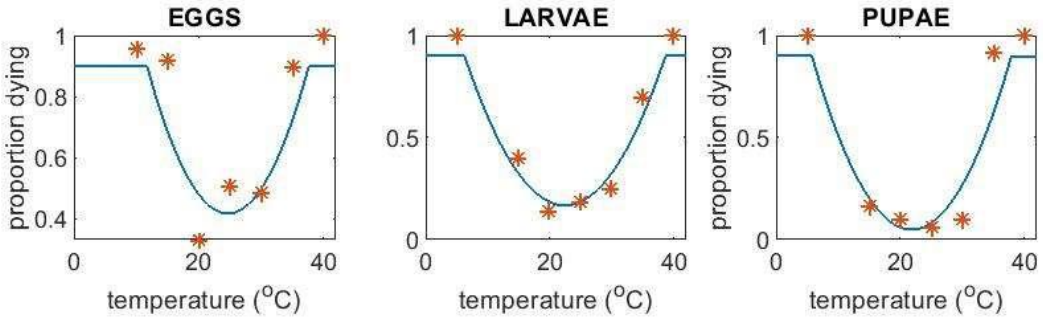

  - Mortality rate described in formula (12).

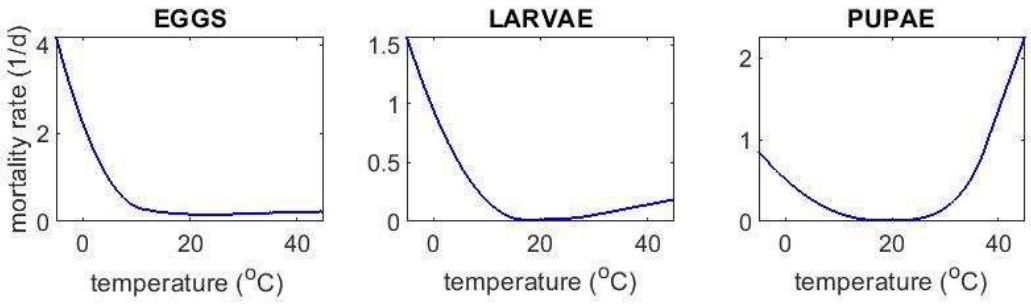

  - Mortality rate for diapausing egg. Continuous line: function $m^{diap}(T) = 0.05301e^{-0.1649T}$. Asterisks: literature data (Thomas et al., 2012).

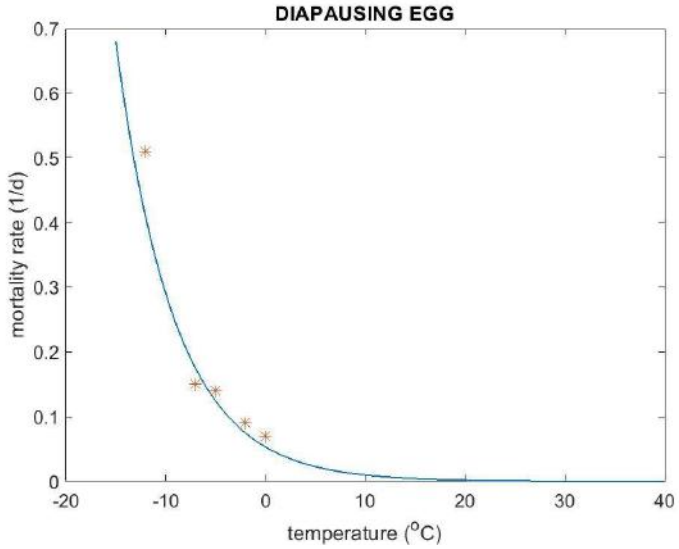

- Fecundity rate. Left panel: fecundity rate function described in formula (14). Right panel: cross section as function of temperature with literature data (asterisks). See Section 2.1.3 for references on data.